Optical and electrical properties of NiO for possible dielectric applications

Authors:
André Venter[1]
Johannes R. Botha[1]

Affiliation:
[1]Department of Physics, Nelson Mandela Metropolitan University, Port Elizabeth, South Africa

Correspondence to:
André Venter

email:
andre.venter@nmmu.ac.za

Postal address:
Department of Physics, Nelson Mandela Metropolitan University, PO Box 77000, Port Elizabeth 6031, South Africa

Dates:
Received: 13 May 2010
Accepted: 21 Sept. 2010
Published: 26 Jan. 2011

How to cite this article:
Venter A, Botha JR. Optical and electrical properties of NiO for possible dielectric applications. S Afr J Sci. 2011;107(1/2), Art. #268, 6 pages. DOI: 10.4102/sajs.v107i1/2.268

Nickel oxide (NiO) is a versatile wide band gap semiconductor material. At present, transparent conducting oxide films find application as transparent electrodes and window coatings for opto-electronic devices but most are *n*-type. However *p*-type conducting films, of which NiO is one, are required as optical windows for devices where minority carrier injection is required. In this study, nickel (Ni) was resistively deposited on glass substrates and oxidised (isochronally) in oxygen at temperatures ranging from 300 ˚C to 600 ˚C. The oxidised Ni layers were subsequently characterised using scanning electron microscopy (SEM), X-ray diffraction (XRD) and UV-visible photospectrometry in the range 200 nm – 1000 nm. The four point probe method (van der Pauw geometry) was used to determine the sheet resistances of the oxidised films. SEM results of the surface revealed a strong dependence of the surface texture and particle size on the oxidation temperature and time. XRD performed on the oxidised Ni indicated progressive transformation from nanograined polycrystalline Ni to NiO at elevated temperatures. Film thicknesses, particle sizes, energy band gap and wavelength-dependent refractive indices were determined from transmission and absorbance data.

Introduction

Nickel oxide (NiO) is a versatile wide band gap semiconductor material. At present, transparent conducting oxide films, such as indium oxide, tin oxide and zinc oxide, are routinely used as transparent electrodes and window coatings for opto-electronic devices.[1,2] These films are *n*-type. However *p*-type conducting films are required as optical windows for devices where hole injection is required. NiO is a *p*-type semiconductor with a band gap ranging from 3.6 eV to 4.0 eV,[3] transparent to ultraviolet (UV), visible and near infrared radiation and consequently has the potential to address this need.[3] A more subtle but equally important potential application of NiO is as an oxide for metal-oxide-semiconductor (MOS) devices.

Recently, $InAs_{1-x}Sb_x$ has emerged as an excellent material for the development of photodetectors and emitters in the near to mid-infrared region (3 μm – 12 μm) of the electromagnetic spectrum. A number of environmentally harmful gas molecules are known to strongly absorb in this region – examples being methane (3.3 μm), carbon dioxide (4.6 μm), NO_x (6.5 μm) and SO_x (7.3 μm), rendering detector devices operating in the 3 μm – 12 μm wavelength region ideal for applications such as optical gas sensing, environmental pollution monitoring and chemical process control.[4] The performance of these devices is, however, related to the nature of defect structures in the material. Deep-level transient spectroscopy is often used to characterise electrically active defects in semi-conducting materials, but requires a space charge region that can be populated and depopulated at will. This is normally achieved through a rectifying Schottky Barrier Diode (SBD) or a *p*-*n* junction device. SBDs, however, are rarely of good quality when fabricated on degenerate narrow band gap materials such as InAs or GaSb. An alternative approach is to use a MOS structure for establishing a space charge region. NiO, as mentioned, can be either a *p*-type semiconductor or it may, depending on the dopant defect concentrations in the material, also be highly resistive. NiO on InAs may therefore, in principle, either produce a *p*-*n* junction or a MOS device, both being suitable rectifying devices for probing the electrically active defects in narrow gap semiconductors. This study was primarily aimed at the development of an oxide (dielectric) of high integrity, to be used in an InAs MOS device.

Experimental set-up

Ni layers, typically 1000-Å thick, were resistively deposited onto 22 mm x 32 mm microscopic glass substrates obtained from Knittel Glaser, Braunschweig, Germany. The glass substrates were cleaned with ultra pure trichloroethylene, acetone and methanol, followed by rinsing successively in deionised water (ρ = 18 MΩcm). The samples were subsequently blown dry with nitrogen prior

to loading into a stainless steel vacuum chamber with a base pressure of 2 x 10^{-5} mbar. The Ni shot (99.99% purity) was resistively heated using an aluminium oxide (Al2O3)-coated tungsten basket. Typical deposition rates were 2 Å/s – 3 Å/s. The Ni layers were subsequently annealed (isochronally) in 99.5% pure oxygen (O_2) for a period of 1 h or 2.5 h (two separate series) in the temperature range 300 ˚C – 600 ˚C. The oxygen flow rate was 200 cm^3/min and the residual ambient gases were carbon monoxide, carbon dioxide, nitrogen and argon. The annealed films were then extensively characterised in order to determine the experimental conditions required for optimal NiO formation.

The structure and crystallinity of the films were investigated by X-ray diffraction (XRD) using a Phillips PW 1729 diffractometer (Einhoven, Holland). Cu Kα radiation was used. The surface morphology of the NiO films was studied by scanning electron microscopy (SEM) and the layer thickness by atomic force microscopy (AFM), while the resistivity was determined using the four point probe method in the van der Pauw geometry. For this purpose, 5 mm x 5 mm samples, with In contacts soldered on at 350 ˚C were prepared. Optical measurements were performed by recording the transmittance and reflectance of the respective films using a UV-visible double beam photospectrometer in the 200 nm – 1000 nm wavelength range. The refractive index (n), the energy band gap (E_g) and the wavelength-dependent refractive index [n(l)] of the oxidised nickel films were subsequently determined from these measurements.

Results

Figure 1 depicts the SEM images of the surface morphology of Ni on glass before and after oxidation for 2.5 h. The image depicted in Figure 1a shows that the as-deposited Ni layer, by comparison to the oxidised layers, is relatively smooth, suggesting that the Ni films grown on the amorphous glass substrates are most probably composed of nanosized Ni crystallites. The layer oxidised at 350 ˚C revealed a rather similar, but somewhat rougher, morphology. At subsequent higher temperatures the surface morphologies became grainier. Evidently, the texture of the oxidised Ni layer depends on the annealing temperature.

XRD spectra obtained from the oxidised Ni films are shown in Figure 2. The results were indexed according to the American Society for Testing and Materials data cards for Ni and various NiO phases. The reference spectrum (not shown) confirmed the presence of nanocrystalline fcc Ni grains, as

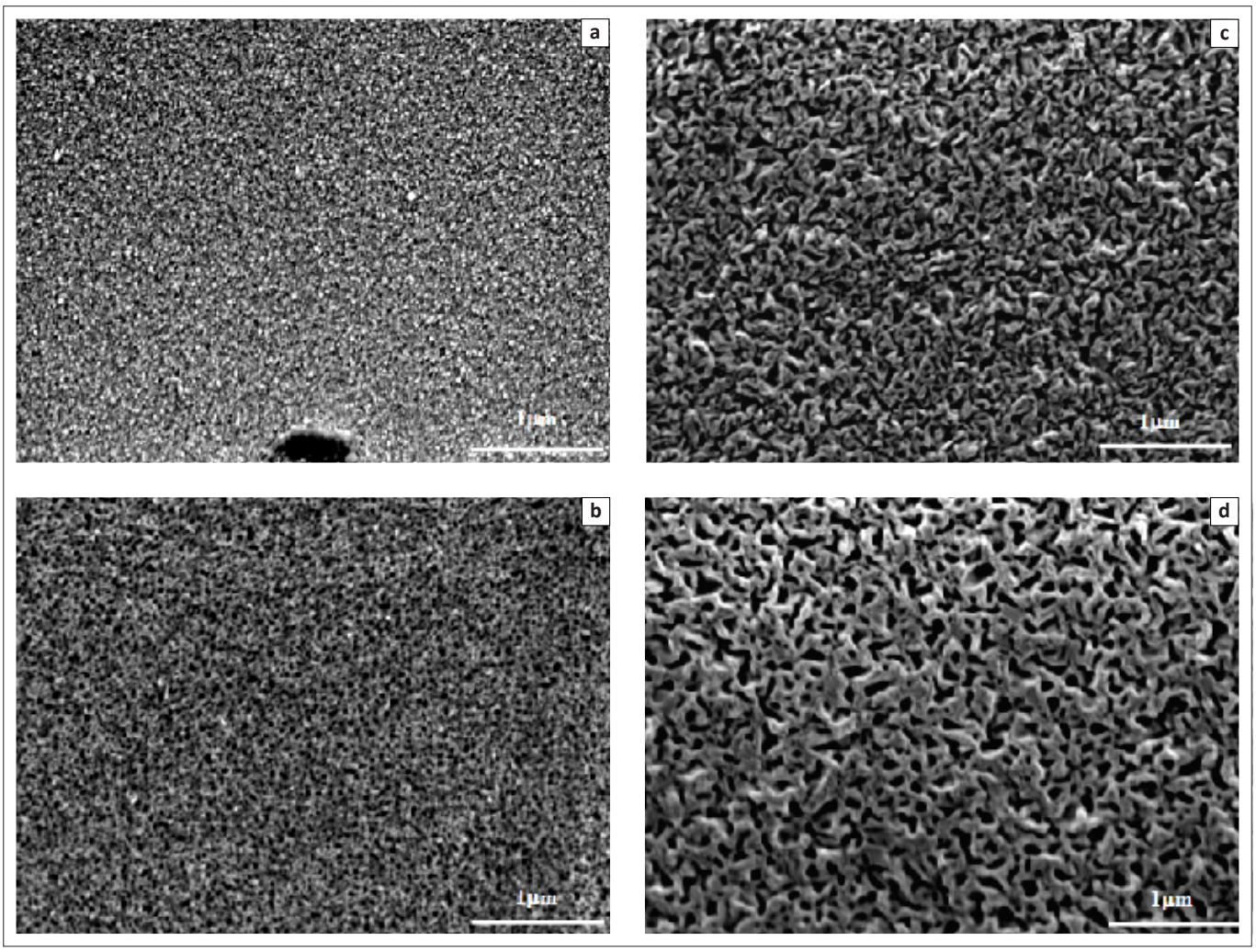

FIGURE 1: Scanning electron microscopy surface morphologies of the Ni films on glass (a) as-deposited and annealed at (b) 350 ˚C, (c) 450 ˚C and (d) 550 ˚C for 2.5 h.

evidenced by the Ni (111) reflection. Ni films oxidised in the temperature range 300 ˚C – 350 ˚C apparently did not oxidise substantially, as only the Ni (111) reflection was observed for these films. Oxidation at temperatures of 400 ˚C and higher resulted in substantial oxidation of the Ni film, with both the (111) and (200) reflection of NiO clearly visible in all the spectra obtained. Evidently, the intensity of these reflections increases with increasing oxidation temperature. No evidence of Ni_2O_3 was found by XRD. This however, does not exclude the possible presence of Ni_2O_3 in amorphous form or in quantities below the detection limit of the XRD system employed in this study. Nel et al.[5] observed similar results and also did not detect any Ni_2O_3, whereas Sasi et al.[3] instead claimed to detect Ni_2O_3 at oxidation temperatures as low as 300 ˚C. These authors deduced their findings from an XPS study, where a broad peak with a binding energy around 856 eV was detected on their sputter-deposited oxidised Ni layers.[6] De-convolution of this peak revealed the presence of NiO, Ni_2O_3 and $Ni(OH)_2$. As in our case, these authors also only detected NiO in their layers when analysed by XRD.[7,8]

An estimate of the crystallite sizes was obtained from the most intense XRD peak [(111) NiO] using Scherrer's equation, while ignoring possible stress-related broadening of the peaks. The particle size L is given by:

$$L = \frac{0.94\lambda}{\omega \cos\theta} \qquad \text{[Eqn 1]}$$

where λ is the X-radiation wavelength, ω the full width at half-maximum (FWHM) and θ the diffraction angle.[9] Figure 3 shows the resultant FWHM and crystallite sizes as a function of the oxidation temperature. In order to determine the relevant FWHM values, a Lorentzian curve was fitted to the respective NiO (111) peaks at each of the oxidation temperatures. For temperatures lower than 400 ˚C, the NiO (111) peaks are poorly defined or completely absent, consequently rendering the determination of particle size at these temperatures impossible. For layers oxidised at temperatures including and exceeding 400 ˚C, the average particle size ranged from approximately 4.5 nm (400 ˚C) to 8.5 nm (550 ˚C). Crystalline 'superior' NiO layers were obtained at an oxidation temperature of 550 °C, corresponding to the largest grain size.

Figure 4 shows the relationship between oxidation temperature and resistivity for these films. It is clear that films annealed for 1 h at a temperature less than 500 ˚C were conductive, with the conductivity decreasing significantly with increasing oxidation temperature. At 500 °C, the resistivity increased to approximately 590 Ωcm, becoming immeasurable when oxidised at 550 ˚C and above. These observations are in agreement with the XRD results, confirming the oxidation of Ni to NiO, a large band gap semiconductor expected to have a large intrinsic resistivity. Ni films annealed for the longer period (2.5 h) followed a similar trend, with layers being oxidised substantially at temperatures as low as 400 ˚C. For this series, the resistivity could only be measured for the films annealed at 350 ˚C and 400 ˚C. The increase in resistivity with oxidation temperature may possibly also be attributed to a decrease in native defects acting as shallow acceptors.[10] The resistivity values obtained for NiO films in this study are in good agreement with reported values, ranging from 10^{-3} to 10^{2} Ωcm.[11,12,13,14] It is instructive to note that Pejova et al.[15], employing the solution growth method, prepared nanocrystalline NiO films with a resistance of several mega ohms and a band gap of 3.6 eV.

The transmittance spectra of the layers oxidised for 1 h and 2.5 h are compared in Figure 5. The transmittance of UV

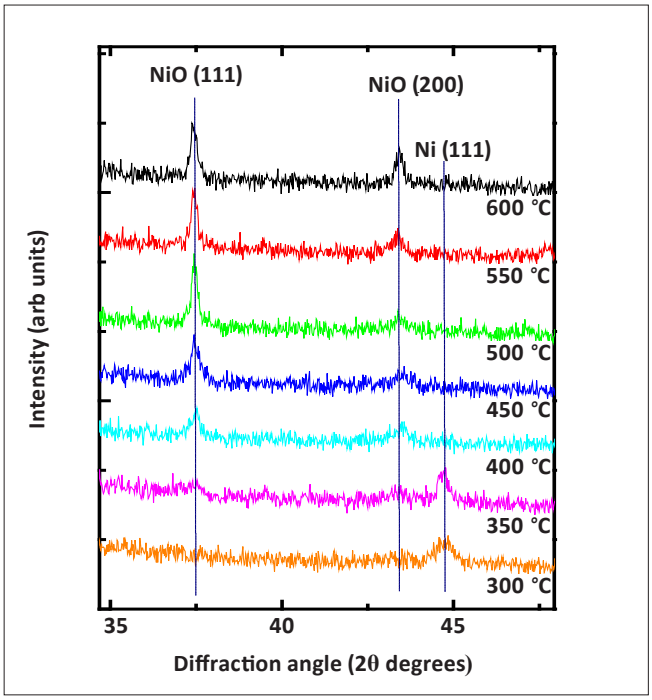

FIGURE 2: X-ray diffraction spectra of Ni films oxidised at various temperatures for 2.5 h.

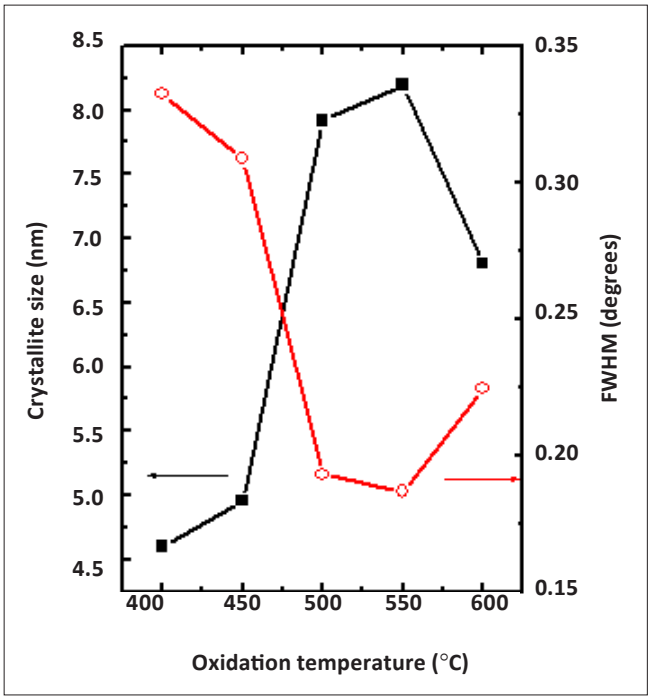

FIGURE 3: X-ray diffraction full-width at half-maximum (FWHM) and crystallite size of Ni films oxidised at different temperatures for 2.5 h.

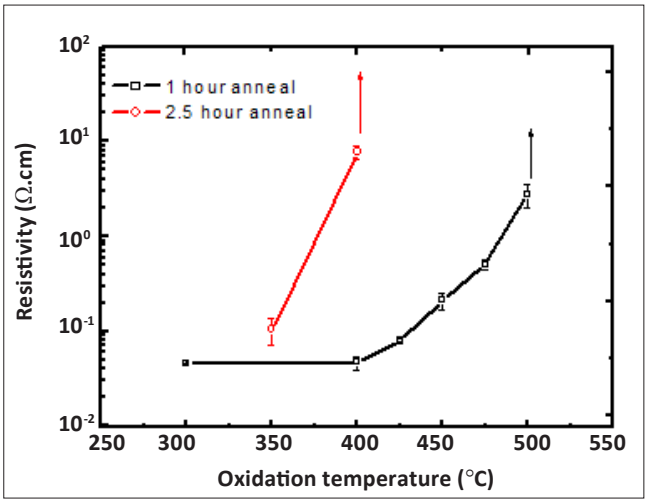

FIGURE 4: Resistivity as a function of the oxidation temperature for Ni films oxidised isochronally for 1 h and 2.5 h in the temperature range 300 °C – 600 °C.

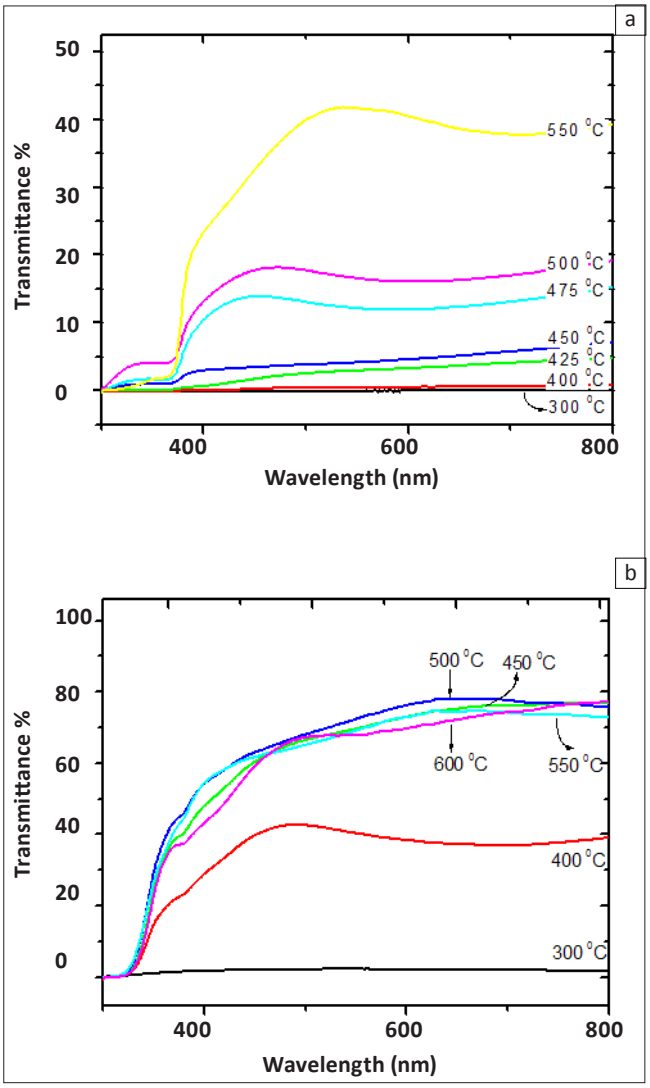

FIGURE 5: Transmittance spectra obtained for Ni films oxidised for a) 1 h and b) 2.5 h.

and visible light through the thin oxidised film is strongly dependent upon the oxidation period and temperature, with the transmittance being insignificant at 350 °C, reaching a maximum of between 70% and 80% in the wavelength range 500 nm – 1000 nm for films oxidised for 2.5 h at 450 °C. This is comparable to, and in some cases exceeds, most transmittance values reported for NiO thin films prepared by similar growth techniques.[12,13,14] An increase in the oxidation temperature to 600 °C had almost no measurable effect on the transmittance. Comparing the transmittance spectra at an oxidation temperature of 450 °C revealed that films annealed for 1 h exhibited a maximum transmittance of approximately half (40%) of that observed for films oxidised for 2.5 h, confirming the transformation from a metal (highly reflective Ni) to a wide band gap semiconductor (transmissive NiO). It is interesting to note that the band edge region showed additional features (Figure 5). These are most probably related to defects in the films.

A simple method for extracting the NiO film thickness and the wavelength dependent refractive index, using either normal incidence transmittance or reflectance for a transparent film on a non absorbing substrate, has been proposed by Sreemany et al.[16] Considering the transmittance data presented in Figure 5, the refractive index n may be determined from the measured absolute transmittance minimum (T_{min} at ~320 nm) provided that the refractive index of the two semi-infinite non-absorbing layers [in this case, n_0 (air) and n_2 (glass)] are known[16]:

$$n = \sqrt{n_0 n_2}\left[\frac{1+\sqrt{1-T_{min}}}{T_{min}}\right] \qquad \text{[Eqn 2]}$$

The film thickness d may then be estimated by:

$$d = \frac{0.25(2m+1)\lambda}{n} \qquad \text{[Eqn 3]}$$

where m is the order of the transmittance minimum and λ the wavelength at which a transmittance (or reflectance) minimum (or maximum) is observed.

Figure 6 shows refractive indices and layer thicknesses as a function of oxidation temperature, obtained from the transmittance spectra shown in Figure 5. For the samples annealed at 450 °C and higher, the inferred refractive index range is 2.2 – 2.5, which is in good agreement with the reported values for NiO.[3] The observed difference in the refractive index values obtained for films in this study is ascribed to either incomplete oxidation or phase transformation or to an uncertainty in the determination of the minimum transmittance wavelength. The layer thicknesses range from ~130 nm to ~280 nm and correlate well with the AFM results. The analytical dispersion equation for thin films on glass substrates was used in this study to determine the wavelength dependent refractive index[17]:

$$n^2(\lambda) = N^2\left[a + \frac{b}{\lambda^2} + \frac{c}{\lambda^4}\right] \qquad \text{[Eqn 4]}$$

where a, b and c are constants to be determined from the refractive indices calculated (as explained above) from the transmittance spectra for the first-, second- and third-order minima, respectively. N is the estimated refractive

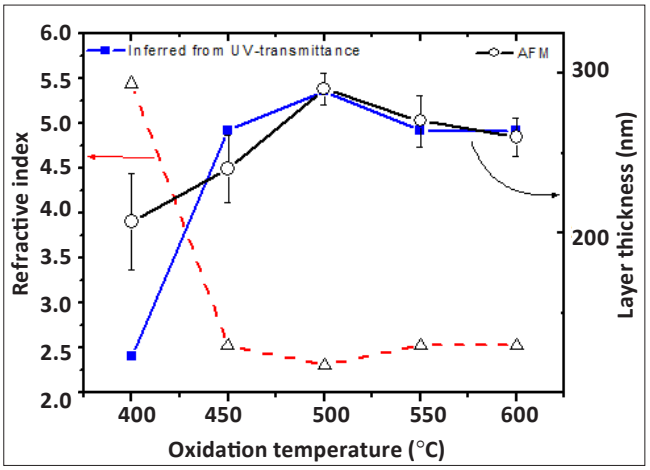

FIGURE 6: Refractive index and layer thickness as a function of oxidation temperature for Ni films oxidised for 2.5 h.

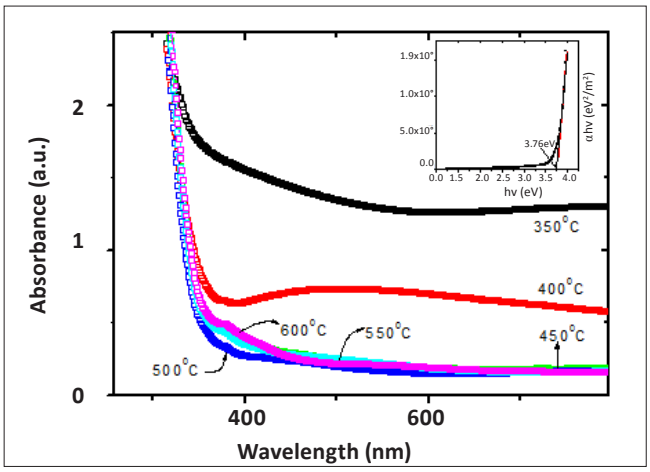

FIGURE 8: Optical absorption spectra for nickel films oxidised for 2.5 h. The inset shows the $(\alpha hv)^2$ versus hv curve for the sample oxidised at 600 °C.

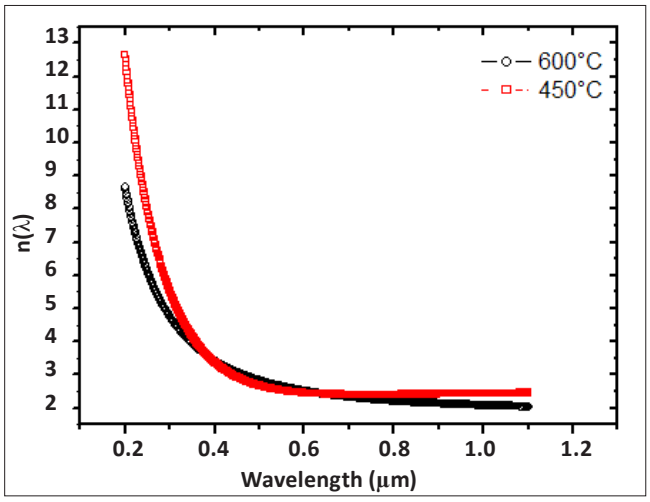

FIGURE 7: Refractive index as a function of wavelength for Ni films oxidised for 2.5 h at 450 °C and 600 °C.

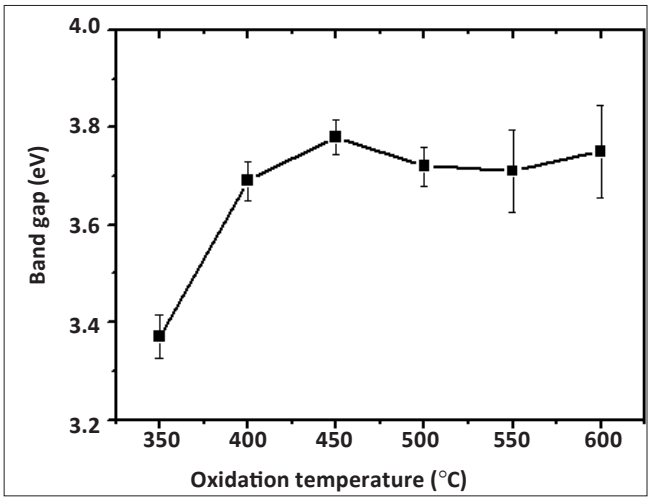

FIGURE 9: Band gap of the oxidised Ni films as a function of oxidation temperature.

index at 550 nm, determined from the dispersion equation by substituting values for $n(\lambda)$ and λ corresponding to the first-order transmission minima of the film. The wavelength dependent refractive index determined in this way is shown in Figure 7.

The absorption co-efficient (α) has been used to determine the band gap of the evolving NiO film by measuring the absorption co-efficient as a function of the incident photon energy (hv). The absorption co-efficient is influenced mainly by scattering losses and fundamental absorption. At shorter wavelengths (close to the optical band gap) scattering can largely be ignored and the absorption co-efficient may be approximated by[18,19]:

$$\alpha = \frac{1}{d} \ln\left[\frac{1}{T}\right] \qquad \text{[Eqn 5]}$$

where d represents the film thickness and T the wavelength-dependent transmittance. A more accurate approach would be to determine the absorption co-efficient from both the reflectance and transmittance data[20]:

$$\alpha = \frac{1}{d} \ln\left[\left[\frac{(C+2R)}{2TR}\right] + \left[\frac{(C+2R)^2}{4T^2R^4} + \frac{1}{R^2}\right]^{1/2}\right]$$

where

$$C = \frac{16 n_1^2 n_2^2}{(n_0 + n_1)^2 (n_1 + n_2)^2} \qquad \text{[Eqn 6]}$$

and n_1 is the refractive index of the oxidised Ni film and n_2 the refractive index of glass. The optical absorption spectra for Ni films oxidised for 2.5 h are shown in Figure 8. Strong absorption is observed in the UV region as a result of the band gap of NiO.

The optical band gap E_g can be determined from the following equation[16]:

$$(\alpha hv)^y = B(hv - E_g) \qquad \text{[Eqn 7]}$$

resulting in $Bhv = BE_g$ when $(\alpha hv)^y = 0$. Here hv is the photon energy, α is the absorption co-efficient, B is a constant related to the material and y is either 2 for a direct transition or ½ for an indirect transition. Figure 8 is a plot of $(\alpha hv)^y$ versus hv for the sample oxidised at 600 °C for 2.5 h. Extrapolating the linear part of the curve in the high-absorption region produces a band gap of approximately 3.76 eV for this NiO film. This value is in excellent agreement with reported

values for NiO films.[3,5,8,10] No linear relation was found for $y = ½$, suggesting that the NiO films in this study all possessed a direct band gap.

Figure 9 shows the relationship between the band gap determined for each of the films annealed for 2.5 h and oxidation temperature. From this graph it is evident that the expected value of 3.7 eV for the band gap is reached after oxidation at or above 400 ˚C, whereafter it remains relatively constant. The slight variation is attributed to the NiO not being completely homogenous, as a result of incomplete phase transformation and/or incomplete oxidation.

Conclusions

Nanocrystalline nickel oxide films were successfully grown on glass substrates, with optimal oxidation of the nickel occurring at temperatures in excess of 450 ˚C for a 2.5 h oxidation period. XRD results confirmed the formation of cubic NiO when oxidised at 400 ˚C or above. The NiO grains apparently had no preferred orientation as both the (111) and (200) reflections were observed in the XRD spectra. Grain sizes, determined from XRD results, ranged from approximately 4.5 nm (400 ˚C) to 8.5 nm (550 ˚C).

Resistivity values obtained for the oxidised Ni films are in good agreement with reported values for films oxidised between 450 ˚C and 600 ˚C. Normal incidence transmittance has been used successfully to extract the optical parameters for the evolving NiO films, including the film thickness and wavelength-dependent refractive index and was found to be very useful in that only the normal incidence transmittance (or reflectance) was required to extensively characterise the evolving NiO in terms of its optical and physical properties.

It was found that the band gap did not significantly change for oxidation temperatures exceeding 400 ˚C for a period of 2.5 h, suggesting that the bulk of the film already consisted of cubic NiO. The band gap ranged from 3.37 eV at 350 ˚C to 3.76 eV at 600 ˚C.

Acknowledgements

This work is based upon research supported by the SA Research Chairs Initiative of the Department of Science and Technology and the National Research Foundation, South Africa, as well as by the Nelson Mandela Metropolitan University. The authors also thank Mr D. O'Connor and Mr J.B. Wessels for technical assistance and Mr J. Jonker for fruitful discussions.

References

1. Gopchandran KG, Joseph B, Abraham JT, Koshy P, Vidyan VK. The preparation of transparent electrically conducting indium oxide films by reactive vacuum evaporation. Vacuum. 1997;48:547.
2. Benny J, Gopchandran KG, Thomas PV, Koshy P, Vaidyan VK. Optical and electrical properties of zinc oxide films prepared by spray pyrolysis. Mater Chem Phys. 1999;58:71.
3. Sasi B, Gopchandran KG, Manoj PK, et al. Preparation of transparent and semiconducting NiO films. Vacuum. 2003;68:149–154.
4. Krier A, Yin M, Smirnov V, et al. The development of room temperature LEDs and lasers for mid-infrared spectral range. Phys Stat Sol A. 2008;205:129.
5. Nel JM, Auret FD, Wu L, Legodi MJ, Meyer WE, Hayes M. Fabrication and characterisation of NiO/ZnO structures. Sens Actuators B. 2004;100:270–276.
6. Zhou Y, Geng Y, Gu D. Influence of thermal annealing on optical properties and surface morphology of NiO_x thin film. Mater Lett. 2007;61:2482–2485.
7. Jiang SR, Yan PX, Feng BX, Cai XM, Wang J. The response of a NiO_x thin film to a step potential and its electrochromic mechanism. Mater Chem Phys. 2003;77:384.
8. Sasi B, Gopchandran KG. Nanostructured mesoporous nickel oxide thin films. Nanotechnology. 2007;18:115613.
9. Cullity DB. Elements of X-ray diffraction. Notre Dame: Addision-Wesley; 1978.
10. Jiang SR, Feng BX, Yan PX, Cai XM, Lu SY. The effect of annealing on the electrochromic properties of microcrystalline NiO_x films prepared by reactive magnetron rf sputtering. Appl Surf Sci. 2001;174:125.
11. Patil PS, Kadam LD. Preparation and characterization of spray pyrolyzed nickel oxide (NiO) thin films. Appl Surf Sci. 2002;199:211.
12. Chen HL, Lu YM, Hwang WS. Thickness dependence of electrical and optical properties of sputtered nickel oxide films. Thin Solid Films. 2006;498:266.
13. Lu YM, Hwang WS, Yang JS, Chuang HC. Properties of nickel oxide thin films deposited by RF reactive magnetron sputtering. Thin Solid Films. 2002;420:54.
14. Sato H, Minami T, Takata S, Yamada T. Transparent conducting *p*-type NiO thin films prepared by magnetron sputtering.Thin Solid Films. 1993;236:27.
15. Pejova B, Kocareva T, Najdoski M, Grozdanov I. Appl Surf Sci. 2000;165:271.
16. Sreemany M, Sen S. A simple spectrophotometric method for determination of the optical constants and band gap energy of multiple layer TiO_2 thin films. Mater Chem Phys. 2004;83:169–177.
17. Anderson O, Bange K, Ottermann C. In: Bach H, Krause D, editors. Thin films on glass. Berlin: Springer-Verlag, 1997; p. 137.
18. Meng LJ, Dos Santos MP. Investigations of titanium oxide films deposited by d.c. reactive magnetron sputtering in different sputtering pressures. Thin Solid Films. 1993;226:22.
19. Aarick J, Aidla A, Kiisller A-A, Uustare T, Sammelselg V. Effect of crystal structure on optical properties of TiO_2 films grown by atomic layer deposition. Thin Solid Films. 1997;305:270.
20. Sujak-Cyrul B, Kolodka B, Misiewics J, Pawlikowski M. Intraband and interband optical transitions in Zn_3AS_2. J Phys Chem Solids. 1982;43(11):1045–1051.